Directed evolution of unspecific peroxygenase in organic solvents

Martin-Diaz, Javier; Molina-Espeja, Patricia; Hofrichter, Martin; Hollmann, Frank; Alcalde, Miguel

DOI
10.1002/bit.27810

Publication date
2021

Document Version
Final published version

Published in
Biotechnology and Bioengineering

Citation (APA)
Martin-Diaz, J., Molina-Espeja, P., Hofrichter, M., Hollmann, F., & Alcalde, M. (2021). Directed evolution of unspecific peroxygenase in organic solvents. *Biotechnology and Bioengineering*, *118*(8), 3002-3014. https://doi.org/10.1002/bit.27810

Promega

Custom Manufacturing Designed to Meet Your Needs

Learn How to Get Exactly What You Need, Delivered Where and When You Need It

40+ years CUSTOM EXPERIENCE

5 GLOBAL Mfg Sites

PRIMARY MANUFACTURER

Your specifications. Your format.
Our scientists waiting to help.

Finding the right supplier for your biotechnology and biopharma products can be a challenge. Partner with Promega and work with a dedicated team of experts willing to provide you with the scientific expertise, ongoing technical support and quality standards to support your success from the first conversation through product delivery.

Let's TALK CUSTOM

Learn more here:
www.promega.com/CustomManufacturing


Custom Manufacturing Services: Exactly What You Need, Delivered Where and When You Need It

Download Our Custom Manufacturing Services White Paper

Received: 23 February 2021 | Revised: 16 April 2021 | Accepted: 30 April 2021

DOI: 10.1002/bit.27810

ARTICLE

BIOTECHNOLOGY AND BIOENGINEERING WILEY

Directed evolution of unspecific peroxygenase in organic solvents

Javier Martin-Diaz[1] | Patricia Molina-Espeja[1] | Martin Hofrichter[2] | Frank Hollmann[3] | Miguel Alcalde[1,4]

[1]Department of Biocatalysis, Institute of Catalysis, CSIC, Madrid, Spain

[2]Department of Bio- and Environmental Sciences, TU Dresden, International Institute Zittau, Zittau, Germany

[3]Department of Biotechnology, Delft University of Technology, Delft, The Netherlands

[4]EvoEnzyme S.L., Parque Científico de Madrid, Madrid, Spain

Correspondence

Miguel Alcalde, Department of Biocatalysis, Institute of Catalysis, CSIC, Cantoblanco 28049, Madrid, Spain.
Email: malcalde@icp.csic.es

Funding information

Ministerio de Ciencia e Innovación, Grant/Award Number: PID2019-106166RB-100-OXYWAVE; Consejería de Educación e Investigación, Grant/Award Number: Y2018/BIO-4738-EVOCHIMERA-CM; H2020 Environment, Grant/Award Number: 886567

Abstract

Fungal unspecific peroxygenases (UPOs) are efficient biocatalysts that insert oxygen atoms into nonactivated C–H bonds with high selectivity. Many oxyfunctionalization reactions catalyzed by UPOs are favored in organic solvents, a milieu in which their enzymatic activity is drastically reduced. Using as departure point the UPO secretion mutant from *Agrocybe aegerita* (PaDa-I variant), in the current study we have improved its activity in organic solvents by directed evolution. Mutant libraries constructed by random mutagenesis and in vivo DNA shuffling were screened in the presence of increasing concentrations of organic solvents that differed both in regard to their chemical nature and polarity. In addition, a palette of neutral mutations generated by genetic drift that improved activity in organic solvents was evaluated by site directed recombination in vivo. The final UPO variant of this evolutionary campaign carried nine mutations that enhanced its activity in the presence of 30% acetonitrile (vol/vol) up to 23-fold over PaDa-I parental type, and it was also active and stable in aqueous acetone, methanol and dimethyl sulfoxide mixtures. These mutations, which are located at the surface of the protein and in the heme channel, seemingly helped to protect UPO from harmful effects of cosolvents by modifying interactions with surrounding residues and influencing critical loops.

KEYWORDS

activity, directed evolution, fungal unspecific peroxygenases, organic solvents, *Saccharomyces cerevisiae*, stability

1 | INTRODUCTION

Fungal unspecific peroxygenases (UPOs, EC 1.11.2.1) are heme-thiolate enzymes that bring together the catalytic attributes of classical peroxidases and P450 monoxygenases (Hofrichter et al., 2020). All UPOs reported to date are considered hybrid enzymes, not only displaying characteristic peroxidase activity (i.e., one-electron oxidations) but also a unique promiscuous peroxygenase activity (i.e., two-electron oxidations along with O-transfer), making these biocatalysts tremendously interesting in synthetic chemistry (Sigmund & Poelarends, 2020; Wang et al., 2017). Importantly, the peroxygenase activity of this enzyme is triggered simply by H_2O_2, which acts as both final electron acceptor and the oxygen source, making UPOs versatile biocatalysts in an ensemble of highly selective C–H oxyfunctionalizations, including: aromatic, alkylic,

(cyclo)aliphatic and heterocyclic hydroxylations; aromatic and aliphatic olefin epoxidations; sulfoxidations; *N*-oxidations; deacylations (C−C bond cleavages); ether cleavages (*O*-dealkylations); *N*-dealkylations; and halide oxidations/halogenations (Hofrichter & Ullrich, 2014). However, the substrates of UPOs are often poorly water soluble, requiring reactions to be performed in organic solvents which, depending on their chemical nature and polarity, may negatively affect the enzyme activity and/or stability, impeding an efficient catalysis. Indeed, the loss of the essential water molecules of the protein shell that occurs when an enzyme is immersed in cosolvents may provoke conformational modifications leading to protein unfolding and denaturation; along with this, the potential competitive inhibitory effect of cosolvents is also an important disturbing factor (Doukyu & Ogino, 2010; Dutta Banik et al., 2016; Klibanov, 2001; Serdakowski & Dordick, 2008; Stepankova et al., 2013).

Protein engineering by directed evolution provides the means to tailor biocatalysts that tolerate organic solvents, with successful case studies having been reported for laccases, P450s, esterases, lipases or proteases, to name just a few (Chen & Arnold, 1993; Moore & Arnold, 1996; Song & Rhee, 2001; Takahashi et al., 2005; Wong et al., 2004; Zumarraga et al., 2007). In previous studies, we evolved the UPO from the basidiomycetous fungus *Cyclocybe (Agrocybe) aegerita* (*Aae*UPO) for heterologous functional expression in yeasts, as well as for diverse applications ranging from the synthesis of agrochemicals to that of pharmaceutical compounds (Hobisch et al., 2020; Molina-Espeja et al., 2017 and references herein). The goal in the current study was to obtain *Aae*UPO mutants by directed evolution that were active and stable in organic cosolvents. To improve the enzyme activity in organic cosolvents, acetone, acetonitrile (ACN) and dimethyl sulfoxide (DMSO) were used during the screening (organic cosolvents of different polarities and chemical nature), while selective pressure was controlled through the gradual enhancement of cosolvent concentrations. Beneficial mutations introduced by conventional directed -adaptive- evolution in *Saccharomyces cerevisiae* (i.e., random mutagenesis and in vivo DNA shuffling coupled to the selection of the fittest) were recombined with a set of neutral mutations taken from a former genetic drift study in which we found several UPO mutants with a noticeable activity improvement in cosolvents (Martin-Diaz et al., 2018). The final variants of this directed evolution process were characterized biochemically, and they show a notable improvement in activity and stability in the presence of high concentrations of organic cosolvents. Ultimately, the effects of these beneficial mutations are considered in the context of the enzyme' structure.

2 | RESULTS AND DISCUSSION

2.1 | Directed evolution strategy

The departure point for this study was PaDa-I, an evolved secretion mutant of *Aae*UPO that carries the mutations F12Y-A14V-R15G-A21D-V57A-L67F-V75I-I248V-F311L (the mutations underlined lie in the signal peptide). While the secretion and activity in aqueous media of PaDa-I improved, its general activity in the presence of high concentrations of organic solvents is poor, like that of the wildtype (wt) *Aae*UPO (Molina-Espeja et al., 2014). To improve the activity of PaDa-I in organic solvents, two generations of directed—adaptive—evolution were carried out by random mutagenesis (*ep*PCR) and in vivo DNA shuffling. Additionally, a final cycle of in vivo site-directed recombination (SDR) was performed aimed at recombining neutral mutations previously discovered by genetic drift that increased activity in the presence of organic solvent (Martin-Diaz et al., 2018) (Figure 1).

To promote activity in diverse types of organic solvents, mutant libraries were screened in the presence of cosolvents of different chemical nature and polarities, with decreasing logP values of −0.24, −0.34, and −1.3, respectively: acetone, ACN and DMSO. The selective pressure was regulated by gradually augmenting the concentration of the organic solvents in each round of directed evolution (see Section 5 for details), establishing a screening threshold based on the percentage of cosolvent at which the parental type retained 1/3 of its activity in aqueous medium. The main selection criterion used was referred to as the tolerance to the organic cosolvent (i.e., the activity retained in cosolvents), represented as the ratio of the activity in the presence of organic solvent to that in the absence of organic solvents (expressed as a percentage). After screening over 7000 clones in two generations of directed evolution, the best selected variant was the 18F6 mutant that carried the new mutations T197A-T198A-V244A-K290R. This variant had moderately improved C_{50} values (the concentration of cosolvent at which the enzyme maintains 50% of its corresponding activity in aqueous solution) of 14%, 10%, 9.5%, and 7% (vol/vol) for acetone, ACN, methanol and DMSO, respectively, as opposed to 10%, 7%, 8.4%, and 2% (vol/vol) of the parental type PaDa-I. These numbers correlate with a C_{50} increase over PaDa-I variant of 1.41-, 1.44- 1.1-, and 3.65-fold for acetone, ACN, methanol and DMSO, respectively.

In a previous work, we carried out a directed UPO evolution experiment by neutral genetic drift, an engineering strategy that allows to introduce neutral mutations, that is, mutations that are neutral in terms of the natural function of the enzyme, but whose gradual accumulation can open new adaptive routes enabling promiscuous activities and stabilities to be displayed. In this neutral genetic drift campaign performed on PaDa-I, we identified several neutral mutations (F191L, S226G, Q254R, S272P, A317D) that enhanced UPO´s activity in cosolvents, despite the fact it was not applied any selection pressure to increase activity in cosolvents but to maintain native activity in aqueous solution (Martin-Diaz et al., 2018). With the aim of fostering epistatic/synergetic effects, this set of neutral mutations was introduced into the 18F6 variant and recombined by in vivo SDR. SDR is based on the homologous DNA recombination apparatus of *Saccharomyces cerevisiae*, allowing mutant libraries to be rapidly constructed and screened by precisely evaluating the effect of mutations/reversions at the positions targeted in a combinatorial manner (Viña-Gonzalez & Alcalde, 2020) (Figure S1). Approximately, 70% of the clones of the SDR mutant library (library size 3500 clones) were functional variants in the

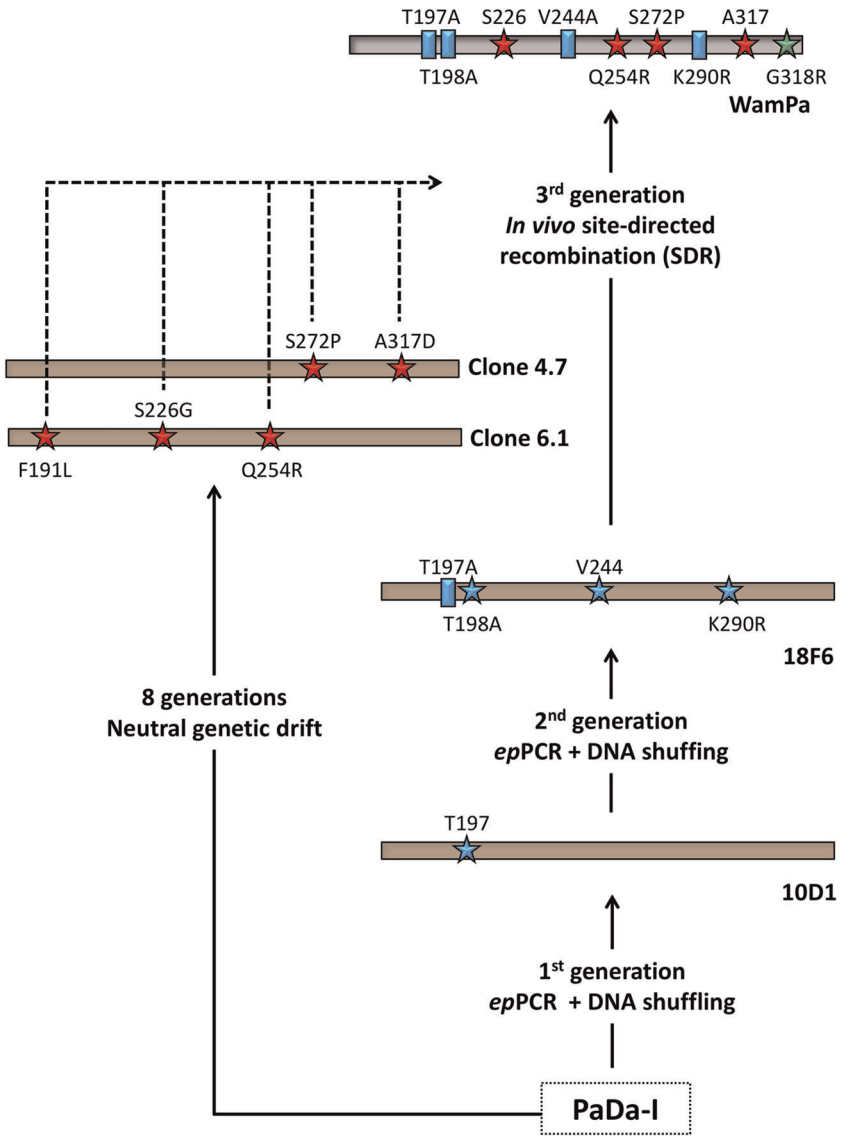

FIGURE 1 Evolution pathway for activity in the presence of organic cosolvents. New mutations are shown as stars, while the previous accumulated mutations are depicted as rectangles. Mutations introduced along the adaptive evolution process are in blue and those in red were obtained by neutral genetic drift. The mutation in green was introduced by a mis-step during PCR amplification [Color figure can be viewed at wileyonlinelibrary.com]

presence of cosolvents, possibly a consequence of the beneficial effects of neutral mutations on the whole mutagenic population. We selected the 13 most promising mutants from this process for a preliminary characterization (Table 1). The best mutant of this set was the WamPa variant, with C_{50} values of 25%, 27%, 14%, and 16% (vol/vol) for acetone, ACN, methanol and DMSO, respectively, as opposed to the values of 10%, 7%, 8.4% and 2% (vol/vol) for the parental PaDa-I. The observed increase in the C_{50} numbers seems to be inversely proportional to the logP of the cosolvents tested (−0.24, −0.34, −0.69, and −1.3 for acetone, ACN, methanol and DMSO, respectively); yet, we cannot establish a clear relationship between the water miscibility of cosolvents and the activity of the enzyme in their presence, taking into account that methanol and DMSO can act as substrate and inhibitor of UPO, respectively. We suspected that such relevant increased of activity in cosolvents had to be related with unique combinations of beneficial mutations from the directed evolution experiment in cosolvents with the neutral ones from the genetic drift campaign. After sequence analysis, we verified that the mutational scaffold of the 18F6 variant (T197A-T198A-V244A-K290R) was maintained in all the final clones, whereas the five neutral mutations were found in different combinations and the mutations S226G, A317D, Q254R, S272P, and F191L were overrepresented in 11, 9, 8, 8, and 3 variants, respectively (Figure 2). Surprisingly, WamPa included an additional beneficial mutation, G318R, introduced due to an error in the PCR amplification. Indeed, the same sequence but without the G318R mutation is present in the 1G9 mutant, which had a lower C_{50} than WamPa but better than that of the parental PaDa-I variant (Table 1 and Figure 2).

2.2 | Biochemical characterization of evolved UPOs

The parental PaDa-I, the 18F6 mutant from second generation and the three best variants from the SDR library (WamPa, 27D5, and 20C4) were produced and purified to homogeneity (Reinsheitszahl

TABLE 1 C_{50} values for the different variants of the evolution route

Mutant	Library creation	Generation	C_{50} (%) Acetone	C_{50} (%) ACN	C_{50} (%) Methanol	C_{50} (%) DMSO
WamPa	SDR	3	24.9	27.0	14.0	15.9
27D5	SDR	3	21.9	19.7	11.1	8.7
20C4	SDR	3	18.8	19.0	11.1	6.9
1B5	SDR	3	17.8	19.3	6.4	6.6
1G9	SDR	3	16.3	18.7	12.4	7.1
1E11	SDR	3	14.8	18.7	8.4	8.3
6G4	SDR	3	17.7	18.3	8.3	6.0
1A3	SDR	3	17.5	17.9	9.1	5.7
1E5	SDR	3	14.1	17.9	6.6	7.4
20E4	SDR	3	18.8	16.8	7.9	8.1
14E10	SDR	3	14.9	11.6	8.2	8.1
42C11	SDR	3	14.7	11.4	9.9	7.1
2A2	SDR	3	11.1	11.6	8.1	7.1
4.7	Neutral drift	8[a]	13.1	20.3	9.7	2.3
6.1	Neutral drift	8[a]	13.2	17.5	9.6	2.8
18F6	*ep*PCR + DNA shuffling	2	14.1	10.1	9.5	7.3
PaDa-I	Parental type	–	10.0	7.0	8.4	2.0

Note: Activity in organic cosolvents was assessed in kinetic mode using the ABTS assay (100 mM sodium phosphate/citrate buffer pH 4.4, 0.3 mM ABTS, and 2 mM H_2O_2) with the corresponding concentrations of organic cosolvent and appropriate dilutions of enzymes. The C_{50} was defined as the concentration of organic cosolvent at which the enzyme showed 50% of the corresponding activity in buffer.

Abbreviations: ABTS, 2,2′-azino-bis-3-ethylbenzothiazoline-6-sulfonic acid; ACN, acetonitrile; DMSO, dimethyl sulfoxide.

[a]Mutants 4.7 and 6.1 were generated after 8 rounds of neutral genetic drift through purifying selection (Martin-Diaz et al., 2018).

value [Rz] ~2). The activity of these pure enzymes was determined in the presence of organic cosolvents and compared to that in aqueous medium. To rule out any possible bias towards the substrate used in the high-throughput screening (HTS) assay (i.e., 2,2′-azino-bis(3-ethylbenzothiazoline-6-sulfonic acid [ABTS], the colorimetric substrate for peroxidase activity), their activity on veratryl alcohol was also measured (a substrate for peroxygenase activity) (Table 2). Regardless of the substrate, WamPa exhibited a high activity in diverse organic cosolvents retaining approximately 7%, 30%, 12%, and 25% of its activity on ABTS in 30% acetone, 30% ACN, 30% methanol and 15% DMSO, as opposed to the 2%, 1%, 6%, and 4% activity of the parental PaDa-I. The 20C4 and 27D5 mutants also outperformed the PaDa-I variant in organic cosolvents, yet to a lesser extent than WamPa. All the variants showed similar tolerance (retained activity in organic solvents) with veratryl alcohol as a substrate, yet these values were generally higher than those obtained with ABTS as a consequence of the amount of enzyme needed for each activity assay (with K_m values of 8 and 0.05 mM, for veratryl alcohol and ABTS, respectively). UPO variants were also very stable at high concentrations of organic cosolvents (Figure 3). After 24 h in the presence of 60% (vol/vol) of the organic cosolvents, the majority of the variants retained at least 50% of their activity, and in some cases hyperactivation was detected over short incubation times.

3 | MUTATIONAL ANALYSIS

The WamPa variant carries nine beneficial mutations that improved its activity and stability in organic solvents (T197A, T198A, S226G, V244A, Q254R, S272P, K290R, A317D, and G318R: the mutations underlined were derived from the directed—adaptive—evolution pathway whereas the rest are neutral mutations included by SDR) (Figure 1). It is notable that three of the mutations introduced by adaptive evolution (T197A, T198A, and K290R) were also found in the aforementioned neutral genetic drift campaign (Martin-Diaz et al., 2018). Rather than serendipity, finding the same mutations using different experimental strategies (i.e., neutral drift vs. adaptive evolution) indicates that both approaches overlap with each other when targeting common biochemical traits. To rationalize the effect of directed evolution, the mutations of the WamPa variant were mapped onto the crystal structure of PaDa-I (PDB accession number 5OXU) (Figure 4). Most of the changes were distributed at the enzyme's surface and remarkably,

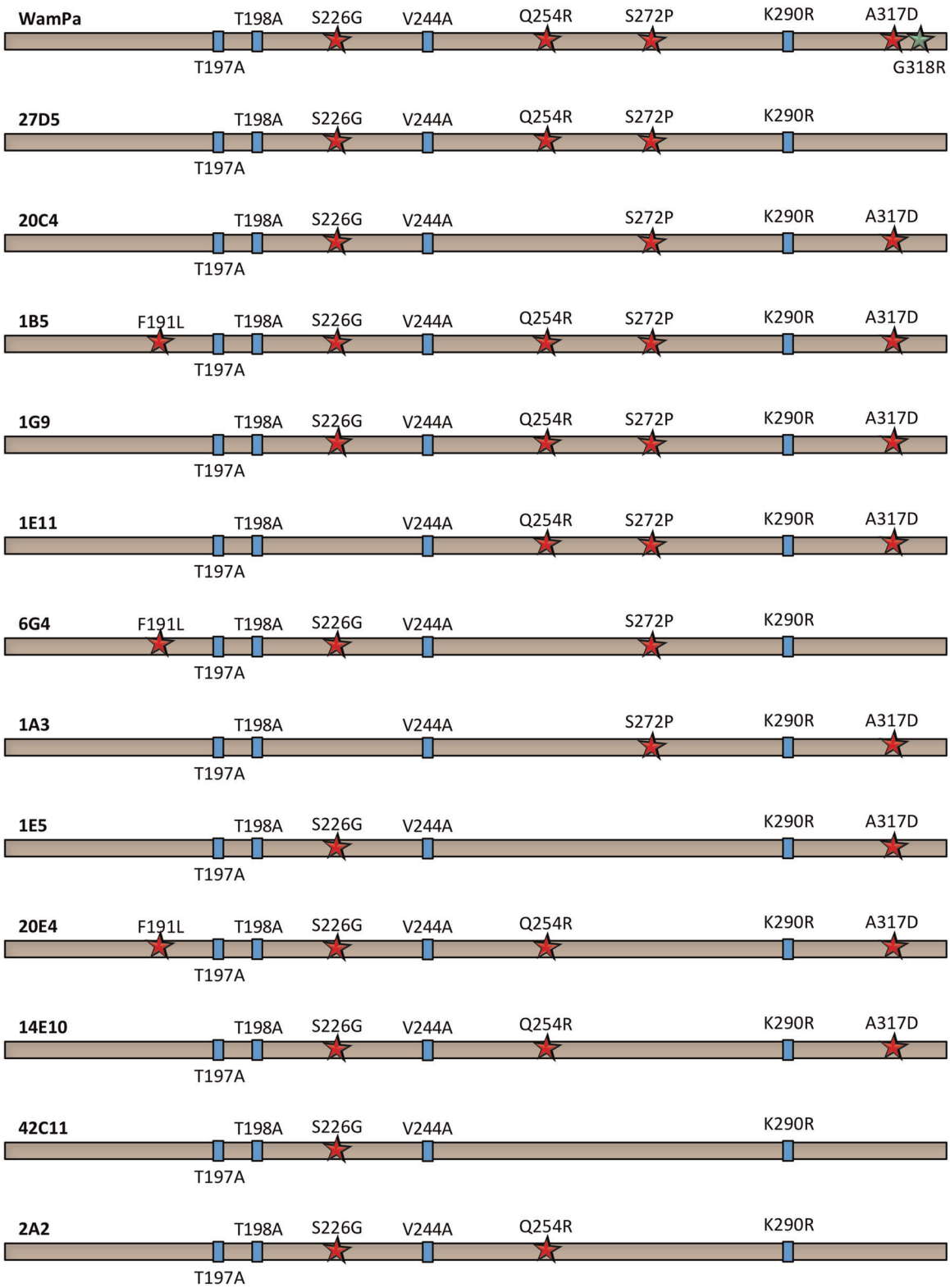

FIGURE 2 Selected mutants from the SDR library. The 18F6 mutant was the scaffold used as the point of departure (T197A, T198A, V244A, and K290R, depicted as blue rectangles) on which the neutral F191L, S226G, S272P, Q254R, and A317D mutations (represented as red stars) and their reversions were evaluated in a combinatorial manner. The green star indicates the G318R mutation introduced by a mis-step in the PCR amplification. SDR, site-directed recombination [Color figure can be viewed at wileyonlinelibrary.com]

TABLE 2 Activity in organic solvents of evolved mutants

Measured with ABTS	Aqueous media		Acetone 30% (vol/vol)[a]			ACN 30% (vol/vol)[a]			Methanol 30% (vol/vol)[a]			DMSO 15% (vol/vol)[a]		
Variant	Activity[b]	Improvement (in fold)[c]	Activity[b]	Improvement (in fold)[c]	Tolerance[d]	Activity[b]	Improvement (in fold)[c]	Tolerance[d]	Activity[b]	Improvement (in fold)[c]	Tolerance[d]	Activity[b]	Improvement (in fold)[c]	Tolerance[d]
PaDa-I	29,854 ± 3965	1.0	704 ± 76	1.0	2.4	410 ± 268	1.0	1.4	1939 ± 72	1.0	6.5	1250 ± 64	1.0	4.2
18F6	28,569 ± 994	1.0	613 ± 66	0.9	2.1	1725 ± 191	4.2	6.0	3148 ± 29	1.6	11.0	5742 ± 44	3.1	20.1
20C4	21,293 ± 1225	0.7	828 ± 224	1.2	3.9	2724 ± 324	6.6	12.8	1925 ± 199	1.0	9.0	3190 ± 86	2.8	15.0
27D5	38,994 ± 422	1.3	1403 ± 589	2.1	3.6	5153 ± 65	12.5	13.2	4111 ± 204	2.1	10.5	9575 ± 91	3.1	24.6
WamPa	32,409 ± 1101	1.1	2299 ± 341	2.4	7.1	9583 ± 748	23.4	29.6	3933 ± 266	2.0	12.1	8168 ± 101	3.0	25.2
Measured with veratryl alcohol	Aqueous media		Acetone 30% (vol/vol)[a]			ACN 30% (vol/vol)[a]			Methanol 30% (vol/vol)[a]			DMSO 15% (vol/vol)[a]		
Variant	Activity[b]	Improvement (in fold)[c]	Activity[b]	Improvement (in fold)[c]	Tolerance[d]	Activity[b]	Improvement (in fold)[c]	Tolerance[d]	Activity[b]	Improvement (in fold)[c]	Tolerance[d]	Activity[b]	Improvement (in fold)[c]	Tolerance[d]
PaDa-I	6457 ± 489	1.0	n.m.	n.m.	n.m.	552 ± 79	1.0	8.6	807 ± 56	1.0	12.5	743 ± 64	1.0	11.5
18F6	6543 ± 827	1.0	n.m.	n.m.	n.m.	1421 ± 99	2.6	21.7	894 ± 181	1.1	13.7	2287 ± 44	3.1	35.0
20C4	6908 ± 119	1.1	n.m.	n.m.	n.m.	2027 ± 387	3.7	29.3	510 ± 83	0.6	7.4	2107 ± 86	2.8	30.5
27D5	7986 ± 67	1.2	n.m.	n.m.	n.m.	2292 ± 148	4.2	28.7	570 ± 137	0.7	7.1	2315 ± 91	3.1	29.0
WamPa	5830 ± 325	0.9	n.m.	n.m.	n.m.	3907 ± 206	7.1	67.0	724 ± 206	0.9	12.4	2262 ± 101	3.0	38.8

Abbreviations: ABTS, 2,2′-azino-bis-3-ethylbenzothiazoline-6-sulfonic acid; ACN, acetonitrile.

[a]The concentration for each organic solvent expressed in molar (M) is:ACN 30% (vol/vol), 5.7 M; acetone 30% (vol/vol), 4 M; DMSO 15% (vol/vol), 2.1 M; methanol 30% (vol/vol), 7.4 M.

[b]Activities are expressed in μmol product/μmol UPO min. Each value, including standard deviation comes from three independent experiments.

[c]The improvement is defined as the ratio of the activity of the corresponding mutant under the conditions specified to that of the parental PaDa-I under the same conditions.

[d]Tolerance in organic cosolvents (i.e., retained activity in cosolvents) is defined as the ratio of the activity in the presence of organic cosolvents to that in the absence of organic cosolvents, given as a percentage. N.m. nonmeasurable—due to the strong background generated by acetone 30% (vol/vol).

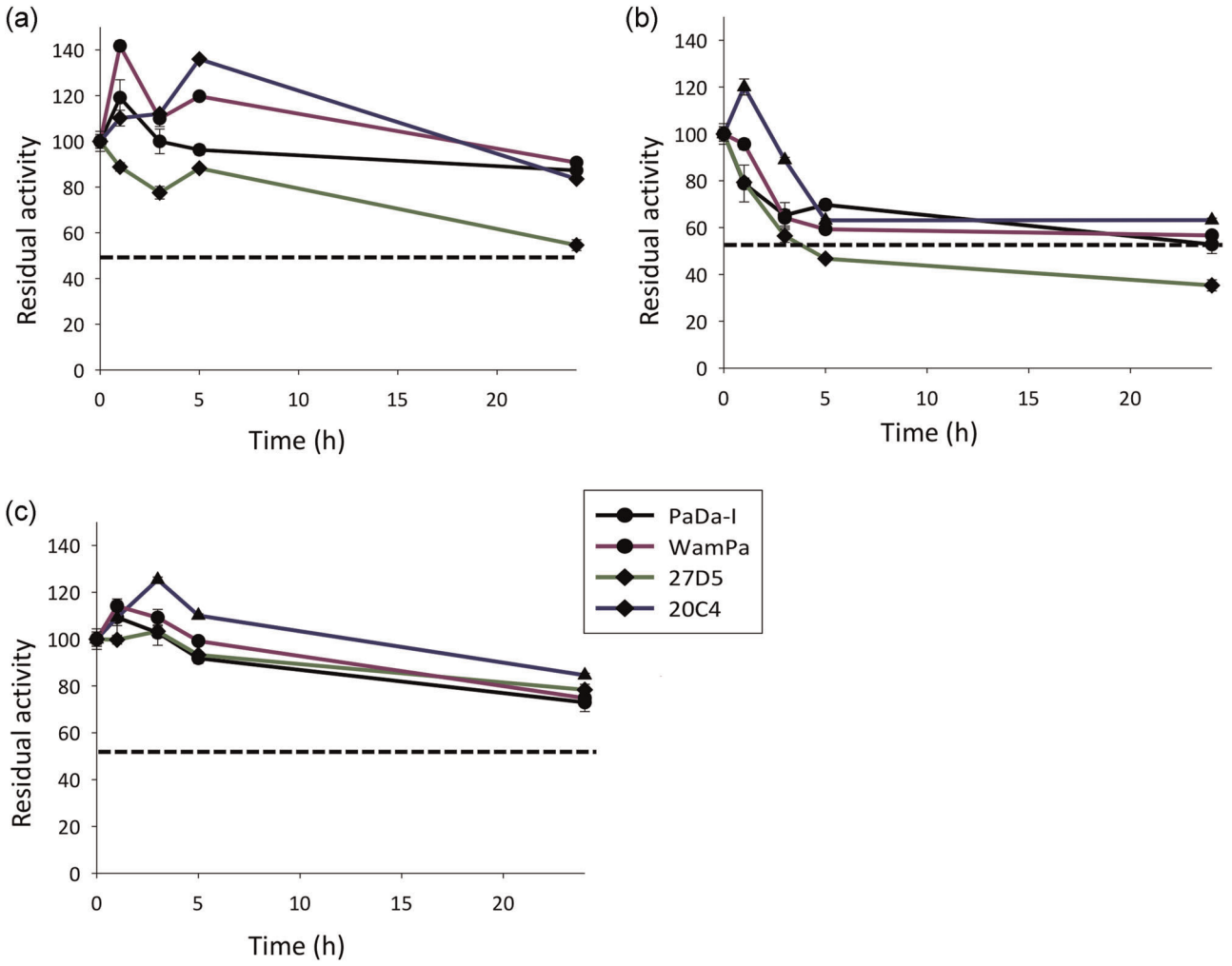

FIGURE 3 Stability in the presence of organic solvents at 60% (vol/vol). Purified enzymes were incubated for 24 h in screw-cap vials with the corresponding cosolvent ([a], ACN; [b], acetone; [c], DMSO). At each time point an aliquot was removed and the enzyme's activity was assessed in an assay with 0.3 mM ABTS and 2 mM H_2O_2 in 100 mM sodium phosphate/citrate buffer (pH 4.4). Residual activity was expressed as the activity in 60% (vol/vol) organic cosolvent relative to the original activity. Each value is represented as the mean and *SD* of three independent experiments. ABTS, 2,2′-azino-bis-3-ethylbenzothiazoline-6-sulfonic acid; ACN, acetonitrile; DMSO, dimethyl sulfoxide [Color figure can be viewed at wileyonlinelibrary.com]

some of them appeared in loops previously identified to be key regions for the enzyme's activity (Ramirez-Escudero et al., 2018). For the sake of clarity, we have distributed the analysis of the mutations into three blocks: surface mutations (S226G, Q254R, S272P, K290R); access to the heme channel (V244A, A317D, G318R); and inner heme channel (T197A, T198A).

3.1 | Surface mutations

The neutral mutations S226G, Q254R, S272P (introduced by SDR) and K290R mutation (introduced by adaptive evolution) were all located at the surface of the protein. The introduction of proline and arginine residues is typically linked with more rigidity and stabilization due to the distinctive cyclic structure of proline's side chain and arginine's positively charged guanidinium group (Doukyu & Ogino, 2010; Lehmann et al., 2020). In particular, the Q254R substitution replaces a neutral (polar) residue with a basic (chargeable) one and according to our model, this mutation could establish a new salt bridge with Asp273 from an adjacent loop that might strengthen this region (Figure 5c,d). The K290R mutation seems to break an H-bond with the Pro324 located in an adjacent helix, concomitantly forming a new H-bond with Asn286 (Figure 5e,f). This local rearrangement seems to produce tighter packing of the surroundings, marked as labile by *B*-factor analysis. The S226G mutation was previously thought to improve thermostability in a structure-guided evolution project (Mate et al., 2017). This substitution is located at a heme Fe^{3+} distance of 12 Å and no effects were observed in the modeling, although replacing a larger, polar alcohol residue (hydroxymethyl group, CH_2–OH) by the smallest nonpolar residue (hydrogen, H) will surely increase hydrophobicity and may imply tighter packing (Figure 5g,h).

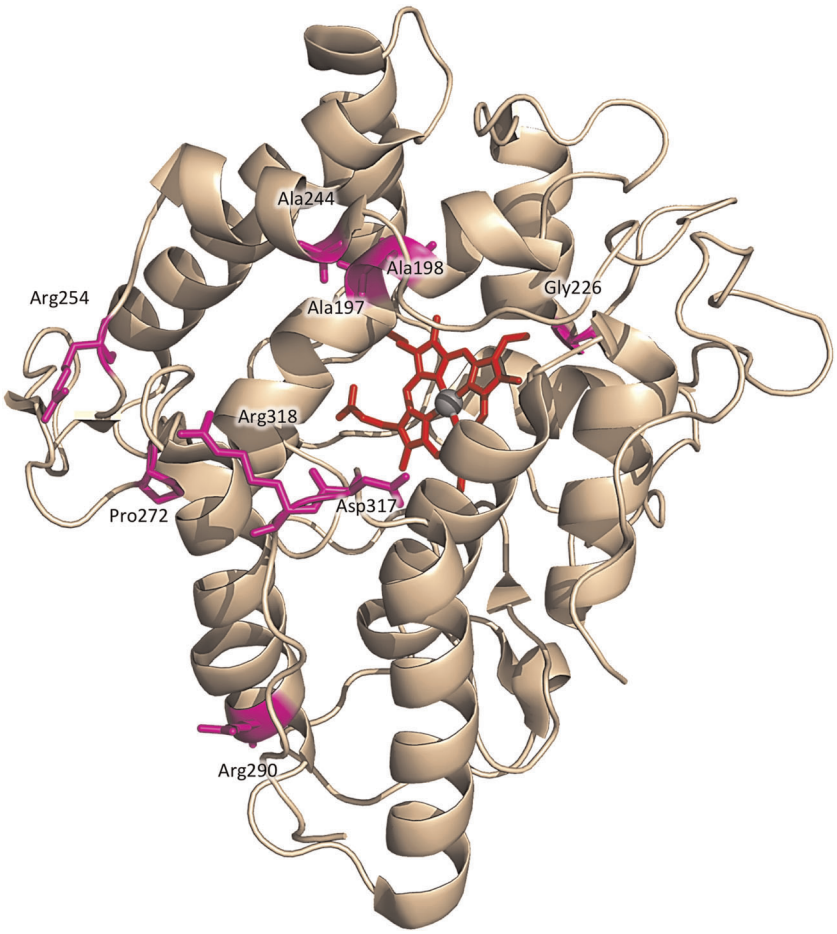

FIGURE 4 General view of the mutations in the WamPa variant. The mutated positions are in pink while the heme is shown in red, with Fe^{3+} in gray. The model was generated by the PyMOL Molecular Graphics System (version 1.6 Schrödinger, LLC) based on the PaDa-I crystal structure (PDB accession number: 5OXU) [Color figure can be viewed at wileyonlinelibrary.com]

3.2 | Access to the heme channel

The V244A mutation lies next to the Ser240-Gly243 loop that is involved in orientating substrates to enter the heme channel through main chain contacts (Ramirez-Escudero et al., 2018) (Figure 5i,j). Indeed, mutations in this region were seen to potentially provoke conformational changes that affect activity and stability in previous directed evolution studies with computational simulations (Molina-Espeja et al., 2016). Thus, replacing valine by alanine (i.e., isopropyl by methyl) just moderately changes hydrophobicity of the respective protein region but efficiently reduces the respective partial molar volume. Conversely, the A317D and G318R mutations (replacing small hydrophobic by larger polar and charged residues) are located in the flexible G314–G318 loop that shapes the heme funnel, which adopts different conformations in the crystal complexes with a panel of UPO substrates (Ramirez-Escudero et al., 2018) (Figure 5i,j). More significantly, previously reported mutations in this loop (e.g., A316P) dramatically improved the enzyme's activity and stability, and hence, this region appears to be fundamental for UPO activity.

3.3 | Inner heme channel

The T197A and T198A mutations were introduced in the first and second generations of adaptive evolution, with notably enhanced activity in the presence of DMSO (Figure 5k,l). Interestingly, both mutations were also detected in several variants obtained by neutral genetic drift, improving activity in the presence of DMSO (Martin-Diaz et al., 2018). Positions 197 and 198 line the inner heme channel and lie next to Phe199 that forms the aromatic triad together with Phe69 and Phe121, a structure that is involved in positioning the substrate at a van der Walls distance from the heme. In previous soaking experiments, we observed a strong inhibitory role of DMSO, which blocks the aromatic triad (Ramirez-Escudero et al., 2018). As such, we can only hypothesize that modifying the residues surrounding Phe199 reduces the residence time of DMSO within the heme channel, although this assumption will have to be demonstrated by future crystallographic and computational work. Furthermore, it can be expected that the replacement of two polar secondary alcohol functionalities (>CH–$O^{\delta-}$–$H^{\delta+}$) by two nonpolar methyl groups (–CH_3) will decrease the overall polarity (and reactivity) of the respective region and hence prevent/reduce possible

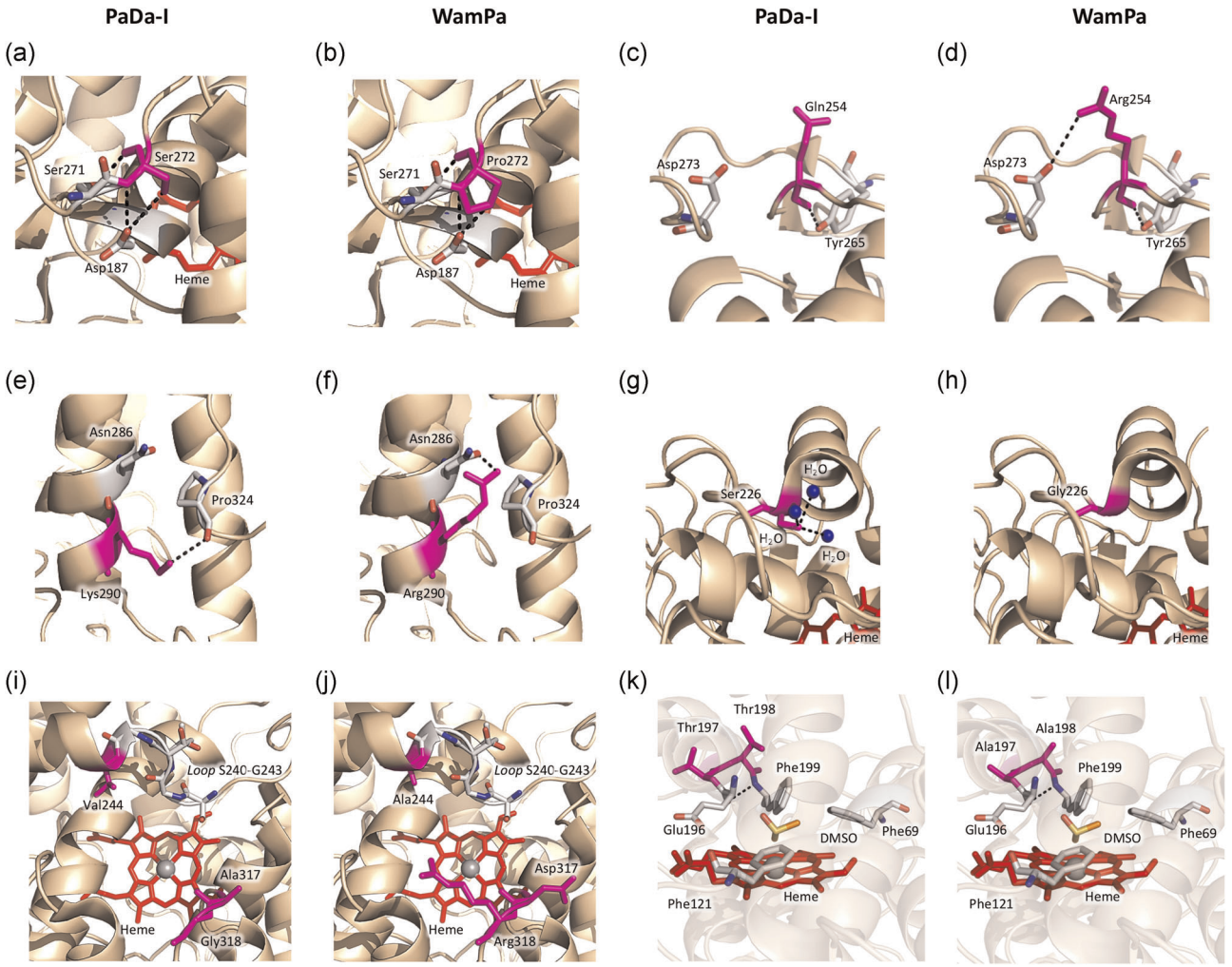

FIGURE 5 Mapping mutations that confer activity in organic solvent. (a–h) Show the UPO surface mutations. (i, j) Show the mutations in the access to the heme channel, whereas (k) and (l) represent the mutations in the inner heme channel. The mutated positions are in pink while the heme is in red with Fe^{3+} in gray. The model was generated with the PyMOL Molecular Graphics System (version 1.6 Schrödinger, LLC) based on the PaDa-I crystal structure (PDB accession number: 5OXU) [Color figure can be viewed at wileyonlinelibrary.com]

inactivating interactions with the strong negative partial charge (δ^-) at the oxygen of DMSO [$(CH_3)_2$–$S^{\delta+}$ = $O^{\delta-}$].

4 | CONCLUSIONS

The new wave of C–H oxyfunctionalization reactions performed by UPOs situate these versatile biocatalysts among the most promising tools for modern synthetic chemistry. However, the hurdles imposed by the poor water solubility of UPO substrates hamper the practical use of these enzymes in a multitude of industrial processes. As the portfolio of substrates and reactions catalyzed by UPO steadily increases, the demand for enzyme engineering strategies that tailor more efficient and active UPOs increases. Here, we have combined directed—adaptive—evolution methods with neutral genetic drift to engineer UPO variants that are active and stable in the presence of high concentrations of organic cosolvents used industrially. These evolved UPOs represent promising departure points to tackle complex oxyfunctionalization chemistry in organic media.

5 | MATERIALS AND METHODS

The *Cyclocybe (Agrocybe) aegerita* UPO mutant PaDa-I comes from previous work (Molina-Espeja et al., 2014). *Saccharomyces cerevisiae* strain BJ5465 was from LGC Promochem, whereas *Escherichia coli* XL1-Blue competent cells were from Stratagene. The expression shuttle vector pJRoC30, with uracil auxotrophy and an ampicillin marker for selection, came from the California Institute of Technology. The restriction enzymes *Bam*HI and *Xho*I were from New England BioLabs. iProof High-Fidelity DNA Polymerase was adquired from Bio-Rad. ABTS, veratryl alcohol, *Taq* DNA polymerase, and yeast transformation kit were purchased from Sigma-Aldrich, Merck. The Zymoprep yeast plasmid miniprep kit and Zymoclean gel DNA recovery kit were from Zymo Research.

The NucleoSpin plasmid kit was purchased from Macherey-Nagel. Oligonucleotides were synthesized by Metabion. All chemicals were of reagent-grade purity.

6 | CULTURE MEDIA

Luria-Bertani (LB) medium was composed of 5 g yeast extract, 10 g peptone, 10 g NaCl, 100 mg ampicillin and *dd*H_2O up to 1 L. Minimal medium was prepared with 100 ml 6.7% yeast nitrogen base, 100 ml 19.2 g/L yeast synthetic drop-out medium supplement without uracil, 100 ml 20% raffinose, 700 ml *dd*H_2O, and 1 ml 25 g/L chloramphenicol. To prepare minimal medium for plates, 100 ml 20% glucose was used instead of 20% raffinose, and 20 g/L of bacto agar were used. Selective expression medium (SEM) contained 100 ml of 6.7% yeast nitrogen base, 100 ml of 19.2 g/L yeast synthetic drop-out medium supplement without uracil, 100 ml of 20% galactose, 67 ml of 1 M KH_2PO_4 buffer pH 6.0, 22 ml of 0.1 M $MgSO_4$, 31.5 ml of absolute ethanol, 1 ml of 25 g/L chloramphenicol, and *dd*H_2O up to 1 liter. Hemoglobin expression medium included 500 ml YP 2X (40 g/L peptone and 20 g/L yeast extract), 66 ml of 1 M KH_2PO_4 buffer pH 6.0, 110 ml of 20% galactose, 22 ml of $MgSO_4$, 31.5 ml of absolute ethanol, 16.5 ml of 20 g/L hemoglobin, 1.1 ml of 25 g/L chloramphenicol, and *dd*H_2O up to 1 L.

7 | DIRECTED EVOLUTION

Three rounds of directed evolution were performed. pJRoC30 was linearized with *Bam*HI and *Xho*I restriction enzymes. The linearized vector was cleaned, concentrated, loaded onto a low-melting-point preparative agarose gel, and purified using the Zymoclean gel DNA recovery kit. Then, the introduction of genetic variability was carried out as described below for each generation, and the PCR products were purified using the Zymoclean gel DNA recovery kit. A total of 200 ng of PCR product (200 ng of each PCR product for the third generation) were mixed with 100 ng of the linearized vector and transformed into competent *S. cerevisiae* cells using the yeast transformation kit. Inserts and linearized plasmid shared approximately 40 bp of homology, to allow recombination and in vivo cloning by the yeast. Transformed cells were plated on minimal medium plates and incubated for 3 days at 30°C, until individual colonies were developed. The oligos used in this study are reported in Table S1.

7.1 | First generation

The PaDa-I variant was used as parental type. Genetic variability was introduced by error-prone PCR (*ep*PCR) using *Taq* DNA polymerase in the presence of $MnCl_2$ as follows: in a final volume of 50 µl, the reaction contained 3% DMSO, 90 nM oligo RMLN, 90 nM oligo RMLC, 0.3 mM deoxynucleoside triphosphates (dNTPs) (0.075 mM each), 0.01 mM $MnCl_2$ (for a mutational rate of 1–3 mutations/kb), 1.5 mM $MgCl_2$, 0.05 U/µl *Taq* DNA polymerase, and 0.14 ng/µl of the parental gene. The parameters fixed in the thermocycler (Mycycler; Bio-Rad) were: 95°C for 2 min (1 cycle); 94°C for 45 s, 55°C for 30 s, and 74°C for 90 s (28 cycles); and 74°C for 10 min (1 cycle). PCR products were mixed with linearized plasmid as described above and subjected to DNA shuffling and cloning upon transformation in yeast.

7.2 | Second generation

The best clone obtained in the first generation, 10D1, was subjected to *ep*-PCR. The mutagenic rates, the PCR conditions, and the thermal-cycling program employed were the same as those described for the first generation. PCR products were mixed with linearized plasmid as described above and subjected to DNA shuffling and cloning upon transformation in yeast.

7.3 | Third generation

The best mutant obtained in the second generation, 18F6, was subjected to SDR in vivo with a palette of neutral mutations (Martin-Diaz et al., 2018). SDR was conducted as reported elsewhere with minor modifications (Viña-Gonzalez & Alcalde, 2020), Figure S1: Six high-fidelity PCR reactions were conducted to amplify the fragments of the gene in a final volume of 50 µl, containing 1% DMSO, 0.5 µM direct primer, 0.5 µM reverse primer, 0.8 mM dNTP (0.2 mM each), 0.5 mM $MgCl_2$, 0.02 U/µl, and 0.2 ng/µl 18F6 template. The primers and parameters fixed in the thermocycler (depending on the fragment to be amplified) were:

PCR 1: RMLN (forward) and CDMR1 (reverse); 98°C for 30 s (1 cycle); 98°C for 10 s, 50°C for 30 s, and 72°C for 15 s (28 cycles); and 72°C for 10 min (1 cycle).

PCR 2: CDMF1 (forward) and CDMR2 (reverse); 98°C for 30 s (1 cycle); 98°C for 10 s, 63°C for 30 s, and 72°C for 15 s (28 cycles); and 72°C for 10 min (1 cycle).

PCR 3: CDMF2 (forward) and CDMR3 (reverse); 98°C for 30 s (1 cycle); 98°C for 10 s, 50°C for 30 s, and 72°C for 15 s (28 cycles); and 72°C for 10 min (1 cycle).

PCR 4: CDMF3 (forward) and CDMR4 (reverse); 98°C for 30 s (1 cycle); 98°C for 10 s, 63°C for 30 s, and 72°C for 15 s (28 cycles); and 72°C for 10 min (1 cycle).

PCR 5: CDMF4 (forward) and CDMR5 (reverse); 98°C for 30 s (1 cycle); 98°C for 10 s, 63°C for 30 s, and 72°C for 15 s (28 cycles); and 72°C for 10 min (1 cycle).

PCR 6: CDMF5 (forward) and CDMR6 (reverse); 98°C for 30 s (1 cycle); 98°C for 10 s, 63°C for 30 s, and 72°C for 15 s (28 cycles); and 72°C for 10 min (1 cycle).

7.4 | HTS assay

Individual colonies were picked and cultured in 96-well microplates (master plates) containing 210 µl of SEM per well. In each

plate, column 6 was inoculated with the corresponding parental and well H1 (containing SEM supplemented with uracil) was inoculated with untransformed *S. cerevisiae* as a negative control. Microplates were incubated at 30°C, at 230 rpm in 80% relative humidity (Minitron; Infors). After 72 h, microplates were centrifuged (Eppendorf 5810 R centrifuge; Eppendorf) for 10 min at 3500 rpm, at 4°C. To determine initial activity (IA), 20 µl of supernatant were transferred to polypropylene microplates with a robotic liquid-handling station (Freedom EVO 100; TECAN), and 180 µl of ABTS reaction mixture (100 mM sodium phosphate/citrate buffer pH 4.4, 0.3 mM ABTS, and 2 mM H_2O_2) were added to each well of the microplates with the help of a pipetting robot (Multidrop Combi reagent dispenser; Thermo Fisher Scientific). The microplates were briefly stirred, and the absorbance was measured in kinetic mode at 418 nm ($\varepsilon_{ABTS}^{\bullet+}$ = 36,000 M^{-1} cm^{-1}) with a microplate reader (SpectraMax Plus 384; Molecular Devices). The values obtained were normalized to those for the corresponding parental type in each microplate. To evaluate the residual activity (RA), master plates were newly replicated as for IA and the reaction mixture was supplemented with 3% DMSO for the first generation, 12% DMSO and 8% acetonitrile (i.e., two replica plates for each master plate; dual screening in cosolvents) for the second generation, and 12% acetonitrile and 18% acetone (two replica plates for each master plate; dual screening in cosolvents) for the third generation. Those clones with IA lower than 50% of the parental activity were discarded, establishing as discriminatory factor among clones the ratio RA/IA.

First rescreening. Aliquots of 5 µl of the best approximately 50 clones of the screening were transferred to new sterile 96-well microplates with 50 µl of SEM per well. Columns 1 and 12 plus rows A and H were not used to prevent the appearance of false positives, column 10, rows D and G (containing SEM supplemented with uracil) were inoculated with parental type and untransformed *S. cerevisiae*, respectively. After 24 h of incubation at 30°C and 220 rpm, 5 µl were transferred to the four adjacent wells containing 205 µl of SEM and further incubated for 72 h. Microplates were assessed using the same activity protocol of the screening described above for each generation.

Second rescreening. An aliquot of 100 µl from the wells with the best approximately 10 clones of first re-screening was inoculated in 3 ml of minimal medium and incubated at 30°C and 220 rpm for 48 h. Plasmids from these cultures were extracted with Zymoprep Yeast Plasmid Miniprep kit. Due to the impurity of the zymoprep product and the low concentration of extracted DNA, the shuttle vectors were transformed into supercompetent *E. coli* cells XL1-Blue and plated onto LB-amp plates. Single colonies were picked and used to inoculate 5 ml LB-amp media and were grown overnight at 37°C and 250 rpm. Plasmids were then extracted by NucleoSpin Plasmid kit and competent *S. cerevisiae* cells were transformed with these plasmids and with the parental type. Five colonies of every single mutant were picked and rescreened as described above for each generation. Parental type and untransformed *S. cerevisiae* were subjected to the same procedure.

8 | PRODUCTION AND PURIFICATION OF EVOLVED VARIANTS

Evolved variants were produced and purified to homogeneity. An individual colony of each selected final variant was inoculated in 20 ml of minimal medium. After 72 h at 30°C and 230 rpm, an aliquot of each culture was transferred to 250 ml of minimal medium to an OD_{600} of 0.3 and further incubated at 30°C and 230 rpm to fulfill two cycles of growth. Then, 50 ml of the culture were used to induce expression of the enzymes in 450 ml of hemoglobin expression medium and incubated at 25°C and 230 rpm until activity reached its maximum (determined with 100 mM sodium phosphate/citrate buffer pH 4.4, 0.3 mM ABTS, and 2 mM H_2O_2). Then, the cultures were centrifuged at 6000 rpm for 30 min at 4°C and the supernatant filtered (nitrocellulose membrane, 0.45 µm pore size). The supernatants were concentrated using a Pellicon tangential ultrafiltration system (10-kDa-cutoff membrane; Millipore) and an Amicon stirred ultrafiltration cell (10-kDa-cutoff membrane; Millipore), followed by diafiltration against 20 mM sodium citrate buffer pH 3.3 (buffer A). The samples were loaded onto two cation-exchange HiTrap SPFF cartridges in a row equilibrated with buffer A (GE Healthcare), connected to an ÄKTA purifier system (GE Healthcare). Proteins were eluted with a 60-min linear gradient from 0% to 40% buffer A containing 1 M NaCl. Fractions with ABTS activity were collected, concentrated, diafiltered against 20 mM Tris-HCl buffer pH 7.8 (buffer B), and loaded onto a BioSuite Q anion-exchange column (Waters) equilibrated with buffer B. Proteins were eluted with a 40-min linear gradient from 0% to 20% buffer B containing 1 M NaCl. The fractions with UPO activity toward ABTS were collected and diafiltered against 10 mM potassium phosphate buffer pH 7.0. Samples of pure enzymes were stored at 4°C. The Rz values (A_{418}/A_{280}) achieved were approximately 2. Throughout the purification protocol, the fractions were analyzed by sodium dodecyl sulfate-polyacrylamide gel electrophoresis on 12% gels, and the proteins were stained with SeeBand protein staining solution (Gene Bio-Application). The concentrations of all crude protein extracts were determined using the Bio-Rad protein reagent, with bovine serum albumin as the standard.

9 | BIOCHEMICAL CHARACTERIZATION OF PURIFIED VARIANTS

9.1 | Activity in the presence of organic cosolvents

Enzyme molarity was adjusted (using 100 mM potassium phosphate pH 7.0 as stability buffer) for every single experiment to obtain linear responses in the measurements. Activity expressed in µmol of product/µmol enzyme per minute, was assessed with ABTS assay (100 mM sodium phosphate/citrate buffer pH 4.4, 0.3 mM ABTS and 2 mM H_2O_2, $\varepsilon_{ABTS}^{\bullet+}$ = 36,000 M^{-1} cm^{-1}, 418 nm) and veratryl alcohol assay (100 mM potassium phosphate buffer pH 7.0, 25 mM

veratryl alcohol and 2 mM H_2O_2, $\varepsilon_{veratraldehyde}$ = 9300 M^{-1} cm^{-1}e's 310 nm), containing 30% (vol/vol) ACN or acetone and 15% (vol/vol) DMSO, and in the absence of organic cosolvent. Every experiment was conducted in triplicate. Tolerance in organic cosolvent (i.e., retained/remaining activity with organic cosolvents) was defined as the percentage of RA in presence of organic cosolvents in relation to the activity in aqueous buffer.

9.2 | Stability in presence of organic cosolvents

Enzyme molarity was adjusted (using 100 mM potassium phosphate pH 7.0 as stability buffer) for every single experiment to obtain linear responses in the measurements. The samples were incubated in sealed vials containing ACN, acetone and DMSO at 60% (vol/vol) and kept at 4°C. Aliquots were withdrawn at 1, 2, 3, 5, and 24 h, and diluted 1:100 with the stability buffer so the concentration of the organic cosolvent (lower than 1%) did not interfere with the measurements. Activity was then determined with the ABTS assay (100 mM sodium phosphate/citrate buffer (pH 4.4), 0.3 mM ABTS, and 2 mM H_2O_2). Every experiment was conducted in triplicate.

10 | DNA SEQUENCING

UPO genes were sequenced by GATC-Eurofins Genomics (Germany). The primers used were RMLN, apo1secdir, apo1secrev, and RMLC, Table S1.

11 | PROTEIN MODELING

The mutations of the final variant, WamPa, were mapped using the crystal structure of the PaDa-I variant from *A. aegerita* (PDB accession number 5OXU) at a resolution of 1.5 Å (Ramirez-Escudero et al., 2018). The model was generated and analyzed by PyMOL Molecular Graphics System, Version 2.0 Schrödinger, LLC.

ACKNOWLEDGMENTS

This work was supported by the by the Bio Based Industries Joint Undertaking under the European Union's Horizon 2020 Research and Innovation program (Grant Agreement No.: 886567, BIZENTE project), the Comunidad de Madrid (CAM) Synergy project Y2018/BIO-4738-EVOCHIMERA-CM, the Spanish Government Projects BIO2016-79106-R-Lignolution and PID2019-106166RB-100-OXYWAVE, the CSIC project PIE-201580E042.

CONFLICT OF INTERESTS

The authors declare the following competing financial interest(s): The UPO variant used in the current study is protected by a CSIC patent WO/2017/081355 (licensed in exclusivity to EvoEnzyme, S.L).

AUTHOR CONTRIBUTIONS

Javier Martin-Diaz performed all experimental work of this article whereas Patricia Molina-Espeja assisted Javier Martin-Diaz in the biochemical characterization of the variants. Martin Hofrichter and Frank Hollmann contributed in the discussion and interpretation of the results. Miguel Alcalde conceived the project, supervised its development and wrote the manuscript, which was reviewed and approved by all the coauthors.

ORCID

Miguel Alcalde http://orcid.org/0000-0001-6780-7616

REFERENCES

Chen, K., & Arnold, F. H. (1993). Tuning the activity of an enzyme for unusual environments: Sequential random mutagenesis of subtilisin E for catalysis in dimethylformamide. *Proceedings of the National Academy of Sciences*, *90*, 5618–5622.

Doukyu, N., & Ogino, H. (2010). Organic solvent-tolerant enzymes. *Biochemical Engineering Journal*, *48*, 270–282.

Dutta Banik, M., Nordblad, J. M., Woodley, G. H., & Peters, A. (2016). Correlation between the activity of candida antarctica lipase B and differences in binding free energies of organic solvent and substrate. *ACS Catalysis*, *6*, 6350–6361.

Hobisch, M., Holtmann, D., Gomez de Santos, P., Alcalde, M., Hollmann, F., & Kara, S. (2020). Recent developments in the use of peroxygenases—Exploring their high potential in selective oxyfunctionalisations. *Biotechnology Advances*, 107615 In press.

Hofrichter, M., Kellner, H., Herzog, R., Karich, A., Liers, C., Scheibner, K., Kimani, V. W., & Ullrich, R. (2020). Fungal Peroxygenases: A Phylogenetically Old Superfamily of Heme Enzymes with Promiscuity for Oxygen Transfer Reactions. In: Ed. Nevalainen, H., *Grand Challenges in Fungal Biotechnology* (pp. 369–403). Springer International Publishing.

Hofrichter, M., & Ullrich, R. (2014). Oxidations catalyzed by fungal peroxygenases. *Current Opinion in Chemical Biology*, *19*, 116–125.

Klibanov, A. M. (2001). Improving enzymes by using them in organic solvents. *Nature*, *409*, 241–246.

Lehmann, M., Pasamontes, L., Lassen, S. F., & Wyss, M. (2020). The consensus concept for thermostability engineering of proteins. *Biochemical and Biophysical Acta*, *1543*, 384–388.

Martin-Diaz, J., Paret, C., Garcia-Ruiz, E., Molina-Espeja, P., & Alcalde, M. (2018). Shuffling the neutral drift of unspecific peroxygenase in *Saccharomyces cerevisiae*. *Applied and Environmental Microbiology*, *84*, e00808–e00818.

Mate, D. M., Palomino, M. A., Molina-Espeja, P., Martin-Diaz, J., & Alcalde, M. (2017). Modification of the peroxygenative:peroxidative activity ratio in the unspecific peroxygenase from *Agrocybe aegerita* by structure-guided evolution. *Protein Engineering, Design and Selection*, *30*, 189–196.

Molina-Espeja, P., Cañellas, M., Plou, F. J., Hofrichter, M., Lucas, F., Guallar, V., & Alcalde, M. (2016). Synthesis of 1-naphthol by a natural peroxygenase engineered by directed evolution. *ChemBioChem*, *17*, 341–349.

Molina-Espeja, P., Garcia-Ruiz, E., Gonzalez-Perez, D., Ullrich, R., Hofrichter, M., & Alcalde, M. (2014). Directed evolution of unspecific peroxygenase from *Agrocybe aegerita*. *Applied and Environmental Microbiology*, *80*, 3496–3507.

Molina-Espeja, P., Gomez de Santos, P., & Alcalde, M. (2017). Directed Evolution of Unspecific Peroxygenase. In: Ed. Alcalde, M., *Directed Enzyme Evolution: Advances and Applications* (pp. 127–143). Springer International Publishing.

Moore, J. C., & Arnold, F. H. (1996). Directed evolution of a para-nitrobenzyl esterase for aqueous organic solvents. *Nature Biotechnology*, *14*, 458–467.

Ramirez-Escudero, M., Molina-Espeja, P., Gomez de Santos, P., Hofrichter, M., Sanz-Aparicio, J., & Alcalde, M. (2018). Structural insights into the substrate promiscuity of a laboratory-evolved peroxygenase. *ACS Chemical Biology*, *13*, 3259–3268.

Serdakowski, A. L., & Dordick, J. S. (2008). Enzyme activation for organic solvents made easy. *Trends in Biotechnology*, *26*, 48–54.

Sigmund, M. C., & Poelarends, G. J. (2020). Current state and future perspectives of engineered and artificial peroxygenases for the oxyfunctionalization of organic molecules. *Nature Catalysis*, *3*, 690–702.

Song, J. K., & Rhee, J. S. (2001). Enhancement of stability and activity of phospholipase A(1) in organic solvents by directed evolution. *Biochimica et Biophysica Acta*, *1547*, 370–378.

Stepankova, V., Bidmanova, S., Koudelakova, T., Prokop, Z., Chaloupkov, R., Jiri, & Damborsky, J. (2013). Strategies for stabilization of enzymes in organic solvents. *ACS Catalisis*, *3*, 2823–2836.

Takahashi, T., Kai-Sing Ng, K., Oyama, H., & Oda, K. (2005). Molecular cloning of the gene encoding vibrio metalloproteinase vimelysin and isolation of a mutant with high stability in organic solvents. *Journal of Biochemistry*, *138*, 701–710.

Viña-Gonzalez, J., & Alcalde, M. (2020). In vivo site-directed recombination (SDR): An efficient tool to reveal beneficial epistasis. In: Ed. Tawfik, D. Ed. Academic Press Elsevier Inc, pp 1-12.

Wang, Y., Lan, D., Durrani, R., & Hollmann, F. (2017). Peroxygenases *en route* to becoming dream catalysts. What are the opportunities and challenges? *Current Opinion in Chemical Biology*, *37*, 1–9.

Wong, T. S., Arnold, F. H., & Schwaneberg, U. (2004). Laboratory evolution of cytochrome P450 BM-3 monooxygenase for organic cosolvents. *Biotechnology and Bioengineering*, *85*, 351–358.

Zumarraga, M., Bulter, T., Shleev, S., Polaina, J., Martínez-Arias, A., Plou, F. J., Ballesteros, A., & Alcalde, M. (2007). In vitro evolution of a fungal laccase in high concentrations of organic cosolvents. *Chemistry and Biology*, *14*, 1052–1064.

SUPPORTING INFORMATION

Additional Supporting Information may be found online in the supporting information tab for this article.

How to cite this article: Martin-Diaz, J., Molina-Espeja, P., Hofrichter, M., Hollman, F., & Alcalde, M. (2021). Directed evolution of unspecific peroxygenase in organic solvents. *Biotechnology and Bioengineering*, 1–13.
https://doi.org/10.1002/bit.27810